Generation and amplification of sub-THz coherent acoustic phonons under the drift of two-dimensional electrons

S. M. Komirenko and K. W. Kim
Department of Electrical and Computer Engineering, North Carolina State University, Raleigh, North Carolina 27695-7911

A. A. Demidenko and V. A. Kochelap
Department of Theoretical Physics, Institute of Semiconductor Physics, National Academy of Sciences of Ukraine, Kiev, 252650, Ukraine

M. A. Stroscio
U.S. Army Research Office, Research Triangle Park, North Carolina 27709-2211
(Received 15 February 2000)

This paper addresses the Čerenkov emission of high-frequency confined acoustic phonons by drifting electrons in a quantum well. We have found that the electron drift can cause strong phonon amplification (generation). The spectra of the confined modes are calculated and their confinement properties are analyzed. The spectra consist of a set of branches, and for each branch, the confinement effect increases considerably when the phonon wave vector increases. We have studied the coupling between electrons and confined modes and proved that the coupling is a nonmonotonous function of the wave vector for each of the phonon branches. We have obtained a general formula for the gain coefficient as a function of the phonon frequency and the structure parameters. For each of the branches, the amplification takes place in a spectrally separated and quite narrow amplification band in the high-frequency range. For the example of *p*-doped Si/SiGe/Si heterostructures it is shown that the amplification coefficients of the order of hundreds of cm^{-1} can be achieved in the sub-THz frequency range.

I. INTRODUCTION

High-frequency coherent phonons have been observed for a number of semiconductor materials and heterostructures: coherent optical phonons have been discovered in GaAs, Ge, Te, as well as in other materials; see Refs. 1 and 2 for a recent review. Short-wavelength acoustic phonons have been studied in bulk GaAs and Si,[3] as well as in Si/Ge, GaAs/AlAs, and $In_xGa_{1-x}N/GaN$ superlattices.[2,4,5] These studies provide information on the excitation mechanisms of the coherent phonons, their dynamics, electron-phonon interactions, and other important phenomena, including phonon control of ionic motion.[6]

Intense coherent phonon waves can be exploited for various applications: terahertz modulation of light, generation of high-frequency electric oscillations, nondestructive testing of microstructures, etc. Usually, both optical and acoustic high-frequency coherent phonons are excited optically by ultrafast laser pulses.[1,2] The development of electrical methods of coherent phonon generation is a long-standing and important problem that has presented many technical challenges.

An electric current flowing though a semiconductor can produce high-frequency coherent acoustic phonons. Two distinct cases can be realized. If the current results from transitions of carriers between bound electron states (so-called hopping transport), the generation of coherent phonons can be achieved if the states are inversely populated.[7] Examples of heterostructures with this type of population inversion include three barrier heterostructures similar to those used in the cascade lasers,[8,9] as well as superlattices with vertical hopping transport.[10]

If the current is due to free electron motion in an electric field, phonon amplification (generation) can be achieved via the Čerenkov effect when the electron drift velocity exceeds the velocity of sound. This effect has been studied intensively for bulk samples.[11] It has been well established that the following three requirements are necessary for practical use of the Čerenkov effect: high electron mobilities, large electron densities, and strong coupling between electrons and amplifying phonons.

Advanced technology of semiconductor heterostructures opens new possibilities to employ the Čerenkov effect, namely, for high-frequency phonon generation. Indeed, two conditions—high electron mobility and large electron densities—are already realized for confined electrons in modulation-doped heterostructures. Then, generally, the electrons are coupled with all phonon modes existing in the sample. However, if there are phonons confined near the location of the electrons, it is obvious that the electrons will be coupled more strongly just with these phonons. Quantum well (QW) structures frequently provide confinement of both electrons and acoustic phonons near the QW layer.[12] For a given QW layer, the phonon confinement increases with the phonon frequency. These properties of quantum heterostructures can facilitate achieving amplification and generation of high-frequency phonons by drifting electrons. This paper addresses the theory of amplification and generation of *confined* acoustic phonons under electron drift in a QW layer. The results are applied to Si-Ge heterostructures.

Since acoustic-phonon confinement is important for our problem we start with a brief analysis of acoustic waves localized within a quantum well layer. Consider the heterostructure shown in Fig. 1, where electrons are confined in

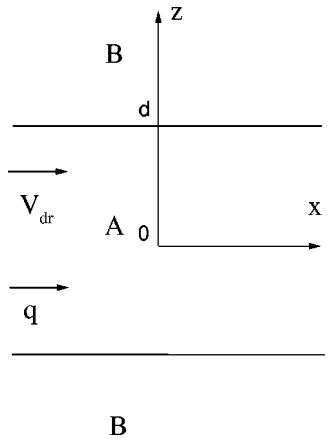

FIG. 1. Geometry of heterostructure analyzed. The quantum well layer and the barrier layers are marked by *A* and *B*, respectively. $\vec{V}_{dr}$ is the electron drift velocity and $\vec{q}$ is the phonon wave vector.

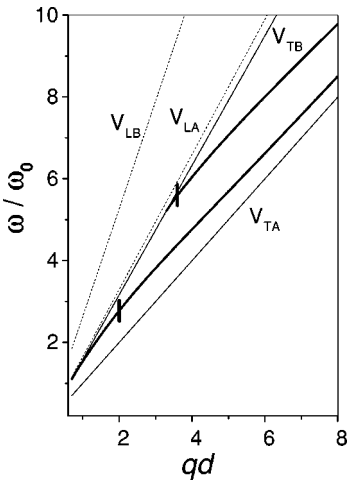

FIG. 2. The dispersion relations for longitudinal and transverse acoustic waves in materials *A* and *B*, and for two lowest SSV confined modes. Results are shown for the strained $Si/Si_{0.5}Ge_{0.5}/Si$ heterostructure. The marks on the curves corresponds to the maxima of the amplification coefficient presented in Fig. 5.

QW layer *A* embedded in a semiconductor material *B*. The thickness of the layer *A* is $2d$. Let isotropic elastic properties be assumed for both materials *A* and *B*. Then, one can characterize them by introducing the longitudinal V_{LA} and V_{LB} and transverse V_{TA} and V_{TB} sound velocities as well as the material densities ρ_A and ρ_B. It is well known that in a layered structure there may exist the effect of localization of acoustic waves within an embedded layer if

$$V_{TA}<V_{TB},V_{LA},V_{LB}; \tag{1}$$

see, for example, Refs. 12 and 13. The localized waves propagate along the layer and decay outside it. There are two classes of the localized waves: shear-horizontal (SH) and shear-vertical (SV). The SH waves are purely transverse and polarized along the layer. Assuming the configuration shown in Fig. 1, the displacement vector for SH waves is $\vec{u}=(0,u_y,0)$. The shear-vertical waves have two projections of the displacement vector: $\vec{u}=(u_x,0,u_z)$.

In this paper we will concentrate on electrons with an isotropic energy dispersion interacting with phonons via the deformation potential. This interaction is dominant in the high-frequency region of interest. For this case, the electrons are coupled only with *longitudinal* lattice vibrations. The SV waves comprise both longitudinal and transverse vibrations, and, thus, are coupled with the electrons. For a given SV wave, the displacement vector can be represented as a sum of longitudinal and transverse components. The relative contribution of the longitudinal component and, hence, the coupling with electrons, depend on the material parameters as well as on the wave vector. The latter can be explained by making use of the sketch of the ω-q diagram shown in Fig. 2 where the dispersion curves of acoustic waves in infinitely extended materials *A* and *B* are shown for typical relations between the velocities

$$V_{TA}<V_{TB}<V_{LA}<V_{LB}. \tag{2}$$

For a localized wave the dispersion relation can be rewritten in terms of factors determining spatial decay of the wave: $\omega^2=V_{LB}^2[q^2-K_{LB}^2(\omega)]=V_{TB}^2[q^2-K_{TB}^2(\omega)]$, where ω and q are the wave frequency and the wave vector, respectively, and $K_{T,L}$ are the frequency-dependent decay factors of longitudinal and transverse components, i.e., $K_{T,L}>0$. This implies that $q^2>(\omega/V_{LB})^2,(\omega/V_{TB})^2$. That is, the waves decaying in material *B* exist only for ω and q to the right of the *TB* line, $\omega=V_{TB}q$, in the ω-q plane. Similarly, one can see that to the right of the *TA* line, $\omega=V_{TA}q$, only interface modes can exist. Thus, the localized waves of interest occur in the sector between the *TB*- and *TA* lines. In Fig. 2, two dispersion branches of these waves are shown. Each of them has a frequency onset. Near the onsets, $q\approx q_\nu$ and $\omega_\nu \approx V_{TB}q$. This implies that outside the QW layer the displacement is almost transversal and decays very slowly in the *B* material. Thus, the relative contribution of the longitudinal component is expected to be small. At $q\gg q_\nu$, when the branch is well developed and $\omega\to V_{TA}q$, the transversal component dominates over the longitudinal component inside the QW layer. As a result, the electron-phonon coupling is expected to have a maximum somewhere in the intermediate region.

Since the heterostructures under consideration are symmetric with respect to the x-y plane, SV waves can be assigned to subclasses of symmetric and antisymmetric waves. Dispersion relations for each class of the waves are represented by a set of branches $\omega=\omega_\nu(q)$, where ν is an integer. Let $\vec{u}_{\nu q}(x,z,t)=\vec{w}_{\nu q}(z)e^{(iqx-i\omega t)}$ be solutions of the elastic equations[14] describing the localized waves. One can show that functions $w_x(z)$ and $w_z(z)$ always have *different* symmetry. We define the symmetric shear-vertical (SSV) modes as those with $w_x(z)=w_x(-z)$, $w_z(z)=-w_z(-z)$ and the antisymmetric ones with $w_x(z)=-w_x(-z),w_z(z)=-w_x(-z),w_z(z)=w_z(-z)$. For a square quantum well, the electrons are coupled only with the SSV-waves.

Solutions with different ''quantum numbers'' $\{\nu,q\}$ are orthogonal. One can normalize the solutions by imposing the condition that for the $\{\nu,q\}$ wave the elastic energy equals $\hbar\omega_\nu(q)$. The set of such solutions (modes) allows one to quantize the lattice vibrations, introduce *confined phonons* and analyze processes of absorption and emission of the

phonons, as well as their amplification and generation under the condition of electron drift. This quantum approach will be explored below.

The rest of the paper is organized as follows. In Sec. II we formulate general equations describing generation and amplification of confined phonons. In Sec. III we present the analytical results based on a simple phonon model, which highlight the general properties of the amplification effect for the confined acoustic phonons. An analysis of a realistic model and its application to particular SiGe heterostructures are given in Sec. IV. The discussion of the results and possible experiments is presented in Sec. VI.

II. THE BASIC EQUATIONS

First we shall define states of the electrons in the QW. Let them be characterized by the subband number l and the two-dimensional wave vector $\vec{k}$. Then the electron wave functions are $\Psi_{l,\vec{k}}(\vec{r},z)=(1/\sqrt{L_xL_y})e^{i\vec{k}\cdot\vec{r}}\chi_l(z)$, where L_y and L_x are the lateral dimensions of the sample. In what follows we assume that only the lowest two-dimensional subband with $l=1$ is populated by the electrons and the energy distances to the next subbands are larger than the energy of the phonons under consideration. In making estimates, we will assume that the barriers confining the electrons are infinitely high, i.e., $\chi_l(z)=(1/\sqrt{d})\cos(\pi zl/2d)$. Electron motion along the QW layer is supposed to be semiclassical and described by a distribution function $F[k_x,k_y]$ dependent on the applied electric field.

As for the phonon subsystem, we shall follow the procedure indicated in Sec. I. First we define the acoustic wave equations[14]

$$\rho_M\frac{\partial^2 u_i}{\partial t^2}-\frac{\partial\sigma_{ij}^M}{\partial x_j}=0,\quad i,j=x,y,z,\quad M=A,B. \tag{3}$$

Here σ_{ij}^M are the stress tensors. For isotropic elastic media σ_{ij}^M are defined through the two Lamè coefficients λ_M and μ_M by

$$\sigma_{z,j}^M=\left(\lambda_M+\frac{2}{3}\mu_M\right)u_{ll}\delta_{ij}+2\mu_M\left(u_{ij}-\frac{1}{3}\delta_{ij}u_{ll}\right), \tag{4}$$

where we use the standard definition for the strain tensor u_{ij}.[14] The Lamè coefficients are related to the longitudinal and transverse sound velocities: $V_{LM}=\sqrt{(\lambda_M+2\mu_M)/\rho_m}$, $V_{TM}=\sqrt{\mu_m/\rho_M}$. At the interfaces, we impose the boundary conditions

$$\vec{u}_B=\vec{u}_A,\quad \sigma_{z,j}^B=\sigma_{z,j}^A \text{ at } z=\pm d. \tag{5}$$

Then, we find solutions of Eq. (3) satisfying conditions $\vec{u}_{\nu q}(z=\pm\infty)=0$. In terms of σ_{ij} and u_{ij} the elastic energy density is $U_{el}^M=\frac{1}{2}\sigma_{ij}^M u_{ij}$. According to the virial theorem the kinetic energy of vibrations equals the potential (elastic) energy. Thus, to normalize a solution, $\vec{u}_{\nu q}$, properly we use the following condition:[15]

$$2L_xL_y\overline{\int_{-\infty}^{\infty}dzU_{el}(z)}=\hbar\omega_{\nu q}, \tag{6}$$

where the overbar means the averaging over one period of the oscillations. In the following sections we will use these equations to compute and study the confined phonon modes in different materials.

The energy of electron-phonon interaction via the deformation potential is

$$H_{int}=b\ \mathrm{div}\,\vec{u}, \tag{7}$$

where b is the constant of the deformation potential. The interaction of the electrons with a given phonon mode $\{\nu,q\}$ should be obtained from Eq. (7) through the substitution $\vec{u}=\vec{u}_{\nu q}$.

Supposing that the electron-phonon interaction is weak we will use the perturbation theory. Then, the transition probabilities for electron states with wave vectors $\vec{k}$ and $\vec{k}'$ due to emission or absorption of the $\{\nu,q\}$ confined phonon mode are

$$P^{(\pm)}(\vec{k},\vec{k}'|\nu,q)=\frac{2\pi}{\hbar}|M(q)|^2\left(N_{\nu q}+\frac{1}{2}\pm\frac{1}{2}\right)\times\delta_{k_y,k_y'}\delta_{k_x\mp q,k_x'}\delta[E(\vec{k})-E(\vec{k}')\mp\hbar\omega_{\nu,q}]\times F(\vec{k})[1-F(\vec{k}')], \tag{8}$$

where $M(q)$ is the matrix element calculated on the wave functions $\chi_1(z)$,

$$M(q)\equiv b\int_{-\infty}^{\infty}\left(iqw_{\nu q,x}(z)+\frac{dw_{\nu q,z}(z)}{dz}\right)\chi_1^2(z)dz, \tag{9}$$

and $N_{\nu q}$ is the phonon occupation number of the $\{\nu,q\}$ mode. In Eq. (8) the upper signs correspond to emission processes, and the lower signs correspond to absorption processes.

We shall mention that Eq. (7) determines interactions between a single electron and the lattice vibrations. If the electron concentration is finite, a perturbation in the form of Eq. (7) drives a spatial redistribution of electrons and thereby leads to screening effects which modify the electron-phonon interaction. This modification can be accounted for in the framework of the standard linear response approach.[16] Taking account for the finite electron concentration leads to a modification of the interaction $H_{int}\to H_{int}^{(scr)}$, as discussed in the Appendix, as well as to the following changes of the above results:

$$|M(q)|^2\to|M^{(scr)}(q)|^2=\frac{|M(q)|^2}{[\kappa^{(el)}(q)]^2} \tag{10}$$

with the electron permittivity $\kappa^{(el)}(q)$ in the form

$$\kappa^{(el)}(q)=1+\frac{2\pi e^2 d}{\kappa}A_{11}(q)\mathcal{B}(qd). \tag{11}$$

Here $A_{11}(q)$ is the polarization operator of two-dimensional electrons:

$$A_{11}(q)=-\frac{2}{L_xL_y}\sum_{\vec{k}}\frac{F(\vec{k})-F(\vec{k}-\vec{q})}{E(\vec{k})-E(\vec{k}-\vec{q})}, \tag{12}$$

κ is the dielectric constant and factor $\mathcal{B}(s)$ is

$$\mathcal{B}(s)=\frac{d^2}{s}\int_{-\infty}^{\infty}\int_{-\infty}^{\infty}d\zeta d\zeta'\chi_1^2(\zeta d)\chi_1^2(\zeta' d)e^{-s|\zeta-\zeta'|}. \tag{13}$$

Now we return to the analysis of Eq. (8). The total rates of emission and absorption of phonons of the $\{\nu,q\}$ mode can be obtained by the summation of Eq. (8) over all initial and final electron states:

$$\mathcal{P}^{(\pm)}(\nu,q)=2\sum_{\vec{k},\vec{k}'}P^{(\pm)}(\vec{k},\vec{k}'|\nu,q), \tag{14}$$

where the factor of 2 results from the electron spin. The sum over $\vec{k}'$ can be computed using the Kroneker δ symbols in Eq. (8). The sum over $\vec{k}$ can be converted into an integral: $\Sigma_{\vec{k}}(\cdots)\rightarrow[L_xL_y/(2\pi)^2]\int dk_xdk_y(\cdots)$. This integral can be simplified by using the energy-dependent δ functions in Eq. (8). Finally, we obtain the emission and absorption rates in the form

$$\mathcal{P}^{(\pm)}(\nu,q)=\frac{m^*}{\pi\hbar^3|q|}\frac{|M(q)|^2}{[\kappa^{(el)}(q)]^2}L_xL_y\mathcal{I}_\nu^{(\pm)}(\vec{q})\times\left(N_{\nu q}+\frac{1}{2}\pm\frac{1}{2}\right), \tag{15}$$

where m^* is the effective mass and the factors $\mathcal{I}_\nu^{(\pm)}$ are:

$$\mathcal{I}_\nu^{(\pm)}(\vec{q})=\int_{-\infty}^{\infty}dk_yF\left[\mathrm{sgn}(q)\frac{m^*\omega_{\nu q}}{\hbar|q|}V_L\pm\frac{1}{2}q,k_y\right]. \tag{16}$$

Here $\mathrm{sgn}(x)=1$ for $x>0$ and $\mathrm{sgn}(x)=-1$ for $x<0$. It is worth noting that in Eq. (15) only the factor $\mathcal{I}^{(\pm)}$ depends on the direction of propagation of the phonon mode.

These results allow one to introduce the kinetic equation for the phonon number of the $\{\nu,q\}$ mode:

$$\frac{dN_{\nu q}}{dt}=\gamma_{\nu q}^{(+)}(1+N_{\nu q})-\gamma_{\nu q}^{(-)}N_{\nu q}-\beta_{\nu q}N_{\nu q}, \tag{17}$$

where $\gamma_{\nu q}^{(\pm)}$ are parameters that determine the evolution of the phonon number $N_{\nu q}$ in time due to the interaction with the electrons. These parameters can be found from Eqs. (15) and (16). The parameter $\beta_{\nu q}$ describes the phonon losses. These losses can include phonon scattering or phonon absorption due to non-electronic mechanisms, phonon decay due to the anharmonicity of the lattice, etc. Equation (17) contains the terms corresponding to spontaneous and stimulated processes. The latter terms can be represented as $\gamma_{\nu q}N_{\nu q}=(\gamma_{\nu q}^{(+)}-\gamma_{\nu q}^{(-)})N_{\nu q}$, with the phonon increment (decrement)

$$\gamma_{\nu q}=\frac{m^*}{\pi\hbar^3|q|}\frac{|M(q)|^2}{[\kappa^{(el)}(q)]^2}L_xL_y(\mathcal{I}_\nu^{(+)}(q)-\mathcal{I}_\nu^{(-)}(q)). \tag{18}$$

Depending on the shape of the electron distribution function, $F(k_x,k_y)$, the value $\gamma_{\nu q}$ can be either positive, or negative. If the phonon increment caused by the electron-phonon interaction is positive and, in addition, it exceeds phonon losses, $\gamma_{\nu q}>\beta_{\nu q}$, the population of corresponding mode(s) should increase in time, i.e., we obtain the effect of phonon generation.

Besides the increment, one can introduce also the amplification (absorption) coefficient for the confined acoustic modes. The amplification coefficient describes the rate of increase per unit length in the acoustic wave intensity $j_{\nu q}$:

$$\alpha=\frac{1}{j_{\nu q}}\frac{dj_{\nu q}}{dx},\quad j_{\nu q}=\hbar\omega\frac{d\omega_{\nu q}}{dq}\frac{N_{\nu q}}{L_xL_y},$$

where $d\omega_{\nu q}/dq$ has the meaning of the group velocity of the corresponding wave. Then, from Eq. (18) we obtain for the amplification coefficient:

$$\alpha_{\nu q}=\gamma_{\nu q}\Big/\left|\frac{d\omega_{\nu q}}{dq}\right|. \tag{19}$$

Obviously, these formulas are valid if $2\pi\alpha/q\ll1$, which always holds, as shown below.

We suppose that the electrons drift in an applied electric field along the QW layer. Under the realistic assumption of strong electron–electron scattering,[17] the distribution function can be thought of in terms of the shifted Fermi distribution:

$$F[k_x,k_y]=F_F\left[k_x-\frac{m^*}{\hbar}V_{dr},k_y\right], \tag{20}$$

where $F_F(\vec{k})=1/(1+\exp[\{E(\vec{k})-E_F\}/k_BT])$ is the Fermi function, E_F is the Fermi level, and V_{dr} and T are the electron drift velocity and temperature, respectively. From Eq. (18), one can see that for the phonons propagating along the electron flux ($q>0$) $\gamma_{\nu q}$, $\alpha_{\nu q}>0$ if the electron drift velocity exceeds the confined-phonon phase velocity:

$$V_{dr}>\frac{\omega_{\nu q}}{|q|}. \tag{21}$$

This criterion is, in fact, the well-known condition of the Čerenkov generation effect.[11] If $q<0$, we always have $\gamma_{\nu q}$, $\alpha_{\nu q}<0$.

Typically, both velocities V_{dr} and $\omega_{\nu,q}/|q|$ are much less than the average electron velocity. This implies that Eq. (20) represents a relatively small disturbance of the Fermi function. Thus, when calculating the screening effect [see Eq. (12)] we can neglect this shift and use just the Fermi function $F_F(\vec{k})$. The shifted distribution, however, has to be taken into account when estimating $\gamma_{\nu q}$ and $\alpha_{\nu q}$.

III. ANALYSIS OF THE SIMPLE MODEL

In this section we analyze the amplification effect for the simplest model of confined phonons. As was discussed above, we shall focus on longitudinal acoustic phonons efficiently interacting with electrons. Hence, we formulate a model for which only longitudinal waves are localized. For

this model we can find analytical results and illustrate the basic properties of the amplification effect. Let us assume that the elastic dilatation moduli λ_M are different for the two materials A and B, while the shear moduli and the densities are equal: $\mu_A=\mu_B$, $\rho_A=\rho_B$. Under this assumption, the longitudinal and the transverse vibrations in the heterostructure are decoupled, which simplifies the analysis considerably. Indeed, the longitudinal vibrations are described by the relative volume change $\mathrm{div}\,\vec{u}$, then Eq. (3) can be presented in terms of $\mathrm{div}\,\vec{u}$:

$$\left[\frac{1}{V_{LM}^2}\frac{\partial^2}{\partial t^2}-\Delta\right]\mathrm{div}\,\vec{u}=0, \quad M=A,B. \tag{22}$$

The boundary conditions at the interfaces (5) can be also formulated for the value $\mathrm{div}\,\vec{u}$:[19]

$$(\lambda_A+2\mu)\mathrm{div}\,\vec{u}|_A=(\lambda_B+2\mu)\mathrm{div}\,\vec{u}|_B \ \text{ at } \ z=\pm d, \tag{23}$$

where $\mathrm{div}\,\vec{u}|_{A,B}$ means the values calculated near the interfaces in materials A,B, respectively. Equations (22) and (23) reduce the problem to the analysis of the value $\mathrm{div}\,\vec{u}$. According to Refs. 12 and 18 in such a simple model the localized SV waves exist if $(\lambda_A+2\mu)/(\lambda_B+2\mu)\equiv h>1$.

Now from Eq. (22) we can find the relative change of the volume to be

$$\mathrm{div}\ \vec{u}(x,y,z)=\begin{cases} iC_A\dfrac{\omega^2}{V_{LA}^2K_{LA}}\cos(K_{LA}z)\exp(iqx-i\omega t), & |z|<d \\ iC_B\dfrac{\omega^2}{V_{LB}^2K_{LB}}\exp(-K_{LB}|z|)\ \exp(iqx-i\omega t), & |z|>d, \end{cases} \tag{24}$$

where

$$K_{LA}(\omega,q)=\sqrt{\frac{\omega^2}{V_{LA}^2}-q^2} \ \text{ and } \ K_{LB}(\omega,q)=\sqrt{q^2-\frac{\omega^2}{V_{LB}^2}}. \tag{25}$$

From Eq. (23) we find that the magnitudes C_A and C_B are related through the equation

$$C_B=-iC_A\sin(K_{LA}d)e^{K_{LB}d}=iC_A\frac{K_{LB}}{K_{LA}}\cos(K_{LA}d)e^{K_{LB}d}. \tag{26}$$

Equation (26) gives the dispersion relation for the localized longitudinal waves:

$$K_{LB}(\omega,q)=K_{LA}(\omega,q)\tan[K_{LA}(\omega,q)d]. \tag{27}$$

It can be rewritten in the parametrical form:

$$\frac{\omega d}{V_{LB}}=\sqrt{\frac{h}{h-1}}\frac{\xi}{|\cos(\xi)|}, \quad qd=\frac{\xi}{\sqrt{h-1}}\sqrt{1+h\tan^2(\xi)}, \tag{28}$$

where ξ is a parameter. From Eq. (27) it follows that $\tan(\xi)>0$ and the allowed values of ξ belong to the intervals

$$\pi\nu\leqslant\xi\leqslant\pi\left(\nu+\frac{1}{2}\right), \quad \nu=0,1,2\ldots. \tag{29}$$

When ξ runs over one of these intervals, the frequency and the wave vector change from

$$\omega=\omega_\nu^0=\pi\nu V_{LB}/d\sqrt{h-1}, \quad q=q_\nu^0=\pi\nu/d\sqrt{h-1},$$

$$\nu=0,1,2\ldots$$

to infinity. We obtain an infinite set of branches $\omega_{\nu q}$ within the sector $qV_{LB}>\omega_{\nu q}>qV_{LA}$. The lowest branch originates from $\omega=0$, $q=0$, while the onsets of the next branches are at finite q_ν^0 and ω_ν^0.

Using Eq. (6) we can normalize the solutions of Eq. (24) and obtain

$$|C_A|^2=\frac{2\hbar}{\rho\omega L_xL_yd}\left(\frac{V_{LA}\xi}{\omega d}\right)^2\frac{\xi\tan(\xi)}{\xi\tan(\xi)+\sin^2(\xi)+\dfrac{1}{h}\cos^2(\xi)}. \tag{30}$$

In Eq. (30) the parameter ξ runs over the νth interval of Eq. (29) for the $\{\nu,q\}$ mode.

Now we can compute the matrix element of Eq. (9) in the explicit form:

$$|M(q)|^2=\frac{2b^2\hbar\omega_\nu(q)}{(\lambda+2\mu)L_xL_yd}f(\xi), \tag{31}$$

$$f(\xi)=\left(\frac{\sin(\xi)}{\xi}\right)^2 \times\frac{\xi\tan(\xi)}{[1-(\xi/\pi)^2]^2\left[\xi\tan(\xi)+\sin^2(\xi)+\dfrac{1}{h}\cos^2(\xi)\right]}. \tag{32}$$

Here, ξ runs in the intervals with $\nu=0,2,\ldots$, otherwise $f(\xi)=0$. The function $f(\xi)$ is strongly correlated with the mode confinement effect: The stronger the confinement, the larger the function $f(\xi)$. This function increases monotonously for the lowest mode, $\nu=0$, and has maxima for excited even modes.

To proceed with the analytical consideration, we consider the low-temperature limit, $T\to 0$. In this case the polarization operator of Eq. (12) and the integrals in Eq. (18) can be calculated:

$$A_{11}(q)=\frac{m}{\pi\hbar^2}\mathcal{A}\left(\frac{q}{2k_F}\right),\quad \mathcal{A}\left(\frac{q}{2k_F}\right)=\left[1-\Theta\left[\frac{q}{2k_F}-1\right]\sqrt{1-\left(\frac{2k_F}{q}\right)^2}\right], \tag{33}$$

$$\mathcal{I}_\nu^{(\pm)}(q)=2k_F\mathcal{J}^{(\pm)}\left(\frac{q}{2k_F}\middle|\frac{V_{dr}}{V_F},\frac{V_{LA}}{V_F}\right),$$

$$\mathcal{J}^{(\pm)}\left(\frac{q}{2k_F}\middle|\frac{V_{dr}}{V_F},\frac{V_{LA}}{V_F}\right)\approx\Theta\left[1-\left(\frac{V_{dr}-\mathrm{sgn}(q)V_{LA}}{V_F}\mp\frac{q}{2k_F}\right)^2\right]\sqrt{1-\left(\frac{V_{dr}-\mathrm{sgn}(q)V_{LA}}{V_F}\mp\frac{q}{2k_F}\right)^2}. \tag{34}$$

Here we suppose that the difference in the elastic moduli is small, $h-1\ll 1$, and that the substitution $\omega_{\nu q}\to V_{LA}q$ can be done under the integrals of Eq. (16). Then, k_F is the Fermi wave vector related to the electron area concentration n through $k_F=\sqrt{2\pi n}$, $\Theta[x]$ is the Heaviside step function and the wave vector q can be of arbitrary sign.

From these last equations we see that in the limit $T\to 0$ the processes of emission and absorption are possible for finite phonon wave vector intervals:

$$-2k_F\left(1-\frac{V_{dr}+V_{LA}}{V_F}\right)\leqslant q\leqslant 2k_F\left(1+\frac{V_{dr}-V_{LA}}{V_F}\right)$$

for emission, (35)

$$-2k_F\left(1+\frac{V_{dr}+V_{LA}}{V_F}\right)\leqslant q\leqslant 2k_F\left(1-\frac{V_{dr}-V_{LA}}{V_F}\right)$$

for absorption. (36)

Since $V_F\gg V_{dr},V_{LA}$, one can estimate the interval of the wave vectors where phonon amplification occurs as $0<q<2k_F$ and determine that the population factor inside this interval is

$$\mathcal{J}^{(+)}(q)-\mathcal{J}^{(-)}(q)\approx\frac{q}{\sqrt{k_F^2-q^2/4}}\frac{(V_{dr}-V_{LA})}{V_F}.$$

The maximum of $\mathcal{J}^{(+)}-\mathcal{J}^{(-)}$ is achieved at the end of the interval given by Eq. (36): $\max(\mathcal{J}^{(+)}-\mathcal{J}^{(-)})\approx 2\sqrt{(V_{dr}-V_{LA})/V_F}$.

Several effects contribute to the phonon increment and the amplification coefficient: the phonon localization effect through the function $f(\xi)$, the screening through the electron permittivity $\kappa^{(el)}(q)$, and the nonequilibrium population of electron states through the factor $(\mathcal{J}^{(+)}-\mathcal{J}^{(-)})$. To represent these factors in an explicit form we rewrite Eq. (19) as follows:

$$\alpha=\frac{\alpha_0 k_F d f[\xi(qd)]}{\left[1+\frac{2d}{a_B}B(qd)\mathcal{A}\left(\frac{q}{2k_F}\right)\right]^2}\times\left[\mathcal{J}^{(+)}\left(\frac{q}{2k_F}\middle|\frac{V_{dr}}{V_F},\frac{V_{LA}}{V_F}\right)-\mathcal{J}^{(-)}\left(\frac{q}{2k_F}\middle|\frac{V_{dr}}{V_F},\frac{V_{LA}}{V_F}\right)\right], \tag{37}$$

where the first multiplier is $\alpha_0(d)=4m^*b^2/\pi(\lambda+2\mu)\hbar^2d^2$ and $a_B=\kappa\hbar^2/e^2m^*$ is the Bohr radius in the material. The rest of the formula depends on three parameters: h, k_Fd, and $(V_{dr}-V_{LA})/V_F$. Using the parametric representation given by Eq. (28), one can compute α either as a function of the phonon wave vector q, or as a function of the frequency ω. Now, we summarize the results for $f[\xi(qd)]$, $\mathcal{B}(qd)$, $\mathcal{A}(q/k_F)$, and $\mathcal{J}^{(\pm)}(q/k_F)$ in order to formulate general features of the amplification effect given by this simple model. The amplification coefficient for the lowest SV mode increases with q (or with ω) and reaches a maximum near the end of the interval of Eq. (36). The rapid increase in $\alpha(\omega)$ is mainly due to the effect of progressive confinement of the phonon mode, while the maximum and following drop in $\alpha(\omega)$ are caused by the abrupt decrease in the population factor $(\mathcal{J}^{(+)}-\mathcal{J}^{(-)})$. Near the maximum the main dependence of α on the electron concentration n comes from the multiplier k_F, i.e., $\alpha\propto\sqrt{n}$. Since the maximum occurs at $qd\approx 2k_F$, for a given electron concentration we find $\alpha_{max}\propto d^{-2}$.

It is worth noticing that this simple model not only represents general features of the amplification effect but also comprises the most favorable conditions for the confinement of longitudinal vibrations. This results in a highest value of the amplification coefficient that could ever be achieved. It is interesting to estimate this upper limit of α. For numerical estimates, we assume the following parameters: $\lambda+2\mu=1.2\times10^{12}$ dyn/cm^2, $V_{LA}=4.7\times10^5$ cm/sec, $h=1.1$, $\kappa=13$, $b=10$ eV, $m=0.067\,m_0$ (m_0 is the free electron mass), $2d=100$ Å, $n=4\times10^{11}$ cm^{-2}. Then we obtain $\alpha_0=6\times10^4$ cm^{-1}, $2k_F=1.6\times10^6$ cm^{-1} and $V_F=2.7\times10^7$ cm/sec. Let us set $(V_{dr}-V_{LA})/V_F=0.05$. Then, the amplification coefficient has a maximum $\alpha_{max}=1.1\times10^3$ cm^{-1} at $\omega=230$ GHz. The corresponding wavelength is 195 Å and the phonon is confined in a spatial region with a thickness of 570 Å.

IV. CALCULATIONS FOR PARTICULAR HETEROSTRUCTURES

Now we return to the more general phonon model formulated in Sec. II and apply it to particular heterostructures. For symmetric SV modes the solution of Eqs. (3) and (4) can be represented as

$$w_x(z)=\begin{cases}C_{LB}e^{-K_{LB}|z|}+C_{TB}e^{-K_{TB}|z|}, & |z|>d\\ C_{LA}\cos(K_{LA}z)+C_{TA}\cos(K_{TA}z), & |z|<d,\end{cases} \tag{38}$$

$$w_z(z)=\begin{cases} i\,\mathrm{sgn}(z)C_{LB}\dfrac{K_{LB}}{q}e^{-K_{LB}|z|}+i\,\mathrm{sgn}(z)C_{TB}\dfrac{q}{K_{TB}}e^{-K_{TB}|z|}, & |z|>d \\ C_{LA}\dfrac{K_{LA}}{q}\sin(K_{LA}z)-C_{TA}\dfrac{q}{K_{TB}}\sin(K_{TA}z), & |z|<d, \end{cases} \tag{39}$$

where $K_{LA}(\omega,q)$ and $K_{LB}(\omega,q)$ are defined by Eqs. (25) and

$$K_{TA}(\omega,q)=\sqrt{\frac{\omega^2}{V_{TA}^2}-q^2}\ \text{ and }\ K_{TB}(\omega,q)=\sqrt{q^2-\frac{\omega^2}{V_{TB}^2}}. \tag{40}$$

The solution given by Eqs. (38) and (39) contains four yet undefined coefficients, C_{LA}, C_{LB}, C_{TA}, and C_{TB}. Then four boundary conditions of Eq. (5) provide a system of four algebraic linear and homogeneous equations, from which one can find relations between the coefficients and an equation for the dispersion relation. The latter equation is a transcendental equation that has to be solved numerically. We have computed the dispersion relations, found the displacement fields, $w_x(z)$ and $w_z(z)$, and analyzed the amplification coefficients for different heterostructures.

Before proceeding with these results we need to make the following remark. The above equations are derived for the model of materials with isotropic elastic properties. To apply the formulas to the cubic crystals we use the so-called isotropic approximation.[20] In this approximation for a material M, the sound velocities V_{LM} and V_{TM} can be expressed in terms of effective moduli: $V_{LM}=\sqrt{(\bar{\lambda}+2\bar{\mu})/\rho}$, $V_{TM}=\sqrt{\bar{\mu}/\rho}$, where $\bar{\lambda}=C_{11}-2C_{44}-4\Delta$ and $\bar{\mu}=C_{44}+\Delta$, with $\Delta=(C_{11}-C_{12}-2C_{44})/5$, and C_{11}, C_{12}, C_{44} are elastic stiffness coefficients of a cubic crystal.

From the analysis given in Sec. III, it follows that the larger acoustic mismatch of materials A and B, the better the phonon confinement and the higher the amplification coefficient. Strained Si/SiGe/Si heterostructures represent a case of practical importance exhibiting considerable acoustic mismatch. It is well established that a thin strained $Si_{1-x}Ge_x$ layer can be embedded between thick Si layers. For example, stable 100-Å SiGe layers with $x\leqslant 0.5$ can be grown by epitaxial processes. These layers are compressively strained and provide good confinement for holes. Due to the compressive character of the strain, the lowest hole subband is assigned to the heavy holes. We have calculated the confined acoustic modes in symmetric Si/SiGe/Si heterostructures and analyzed the Čerenkov effect caused by the drift of the heavy holes in the SiGe QW's.

To calculate the stiffness coefficients C_{ij} for the $Si_{1-x}Ge_x$ layer we use the linear approximation: $C_{ij}^{\mathrm{SiGe}}=(1-x)C_{ij}^{\mathrm{Si}}+xC_{ij}^{\mathrm{Ge}}$; accordingly, $\rho_{\mathrm{SiGe}}=(1-x)\rho_{\mathrm{Si}}+x\rho_{\mathrm{Ge}}$. For example, for $x=0.5$ in the isotropic approximation; this gives $V_{LA}=5.64\times10^5$ cm/sec, $V_{TA}=3.42\times10^5$ cm/sec, while for Si we obtain $V_{LB}=9\times10^5$ cm/sec and $V_{TB}=5.4\times10^5$ cm/sec. Here and in the subsequent discussion we use the stiffness constants, the material densities and other parameters given in Ref. 21. The effective mass for the heavy holes in the SiGe QW is taken to be $m^*=0.4\,m_0$.

In computing localized acoustic waves we found that for any composition of the SiGe layer the lowest branch of the SV waves corresponds to *antisymmetric* SV waves that do not interact with the carriers. *Symmetric* SV waves are always represented by the *excited* branches of the dispersion relations and, hence, always characterized by the previously-discussed onsets of the wave vectors and frequencies. Let us introduce the dimensionless frequency ω/ω_0 with $\omega_0=V_{TA}/d$, and wave vector qd. One can show that in terms of these dimensionless quantities the dispersion relations do not depend on the half-thickness of the layer d. Figure 2 shows just the two lowest SSV phonon branches ω/ω_0 and qd, which correspond to amplification maxima are marked on each branch. The displacement fields w_x and w_z calculated for the lower SSV branch at the marked point are represented in Fig. 3(a) as functions of the transverse coordinate z/d. One can see that the displacements of the lattice are indeed confined near the layer: The displacement w_x is confined mainly inside the layer, while the displacement w_z is confined near the interfaces. In Fig. 3(b) we depict the elastic energy density of this wave as a function of z/d. The complex redistribution of the elastic energy across the structure is due to the fact that the wave under consideration corresponds to the excited phonon branch. From this figure we can conclude that the energy of the wave is confined to a narrow spatial region of thickness of about $4d$.

The magnitude of the interaction strongly depends on the relative change of the volume associated with the displacement wave, $\mathrm{div}\,\vec{u}$. Figure 3 (c) shows the distribution of this quantity across the structure. In Sec. I we presented a qualitative analysis of the relative contributions of both longitudinal and transverse components of the confined phonons. As was discussed, the redistribution between these components gives rise to nontrivial behavior of the electron-phonon coupling as a function of the wave vector or frequency. The coupling is represented by the matrix element of Eq. (9). In Fig. 4 the square of this matrix element is depicted as a function of q for the two lower SSV phonon branches. The result clearly demonstrates the following effects: the wave vector onset, the strong q-dependence and the existence of a maximum of the electron-phonon coupling. Surprisingly, the electron-phonon coupling for the second SSV branch reaches larger values than that of the first. We calculated $w_x(z)$, $w_z(z)$ and $\mathrm{div}\,\vec{u}(z)$ for the second branches and found two physical reasons for this larger coupling. First, it turns out that the magnitudes of the waves of the second branch are larger as a result of the larger ω in the normalization condition of Eq. (6). Second, the longitudinal component of the vibrations and $\mathrm{div}\,\vec{u}$ are more localized inside the QW layer.

To compute the amplification coefficient of Eqs. (18) and (19) we assume that $2d=100$ Å and that the carriers are drifting with velocity $V_{dr}=2.5V_{TA}$. For this value of V_{dr},

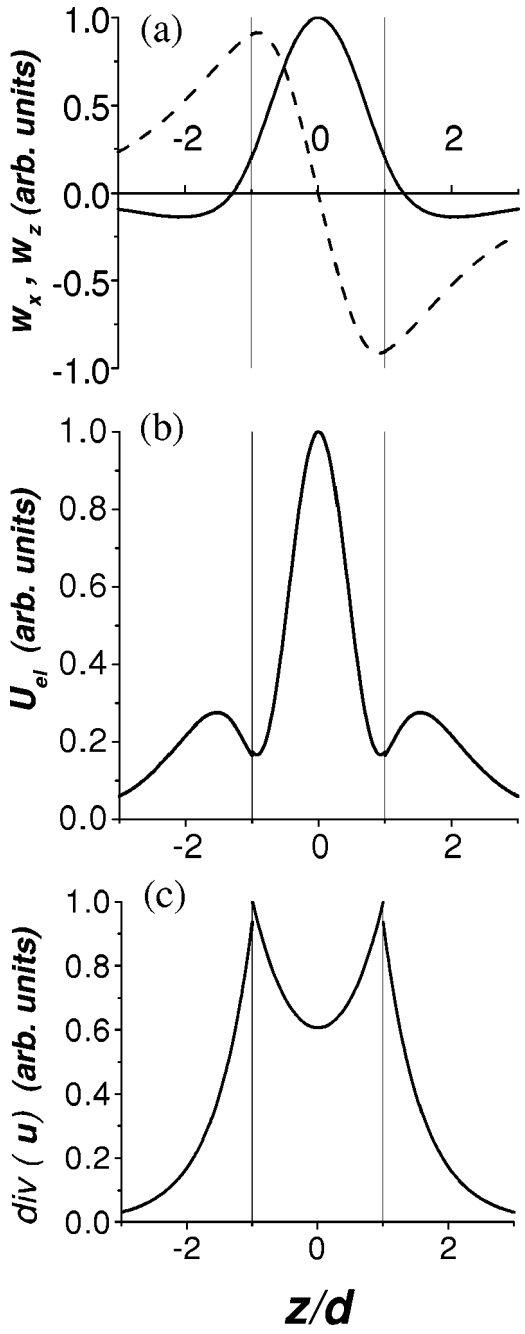

FIG. 3. (a) Displacement fields $w_x(z/d)$, $w_z(z/d)$. (b) Distribution of the elastic energy $U_{el}(z/d)$. (c) div $\vec{u}$ as a function of z/d. The results are presented for the lower SSV phonon branch at the values of ω and q marked in Fig. 2.

the Čerenkov criterion of Eq. (21) is fulfilled for any branch of the confined acoustic modes. The calculations of the amplification coefficient, α, as a function of the phonon frequency, ω/ω_0, are presented in Fig. 5 for the first and second SSV phonon branches. For this particular case, we obtain $\omega_0 = 110$ GHz. The results are calculated for different temperatures: $T = 50$, 100, 150, and 300 K. Now we can see that for each SSV phonon branch the amplification exists in a spectral band. The low-frequency cutoff of the amplification is due to the onset of the phonon branch. The maximum of the amplification coefficient and its high-frequency cutoff are determined by two effects. These are the nonmonotonous

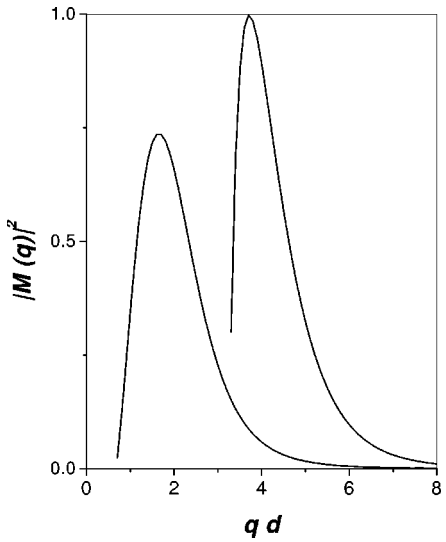

FIG. 4. The square of the matrix elements as a function of qd for two lowest SSV confined phonon branches shown in Fig. 2.

dependence of the electron-phonon coupling on q and ω as well as the decrease in the population factor, $\mathcal{I}^{(+)} - \mathcal{I}^{(-)}$, when the wave vector increases. The population factor is shown in the inset to Fig. 5 as a function of qd for the lower SSV phonon branch at four previously mentioned temperatures. This factor is calculated for both signs of q, i.e., for phonons propagating along the electron drift and those moving in the opposite direction. The occurrence of the onsets is caused by the functional dependences of the integrals of Eq. (16) $\mathcal{I}_\nu^{(\pm)}(q)$ on $\omega_{\nu q}$. A decrease in the population factor for

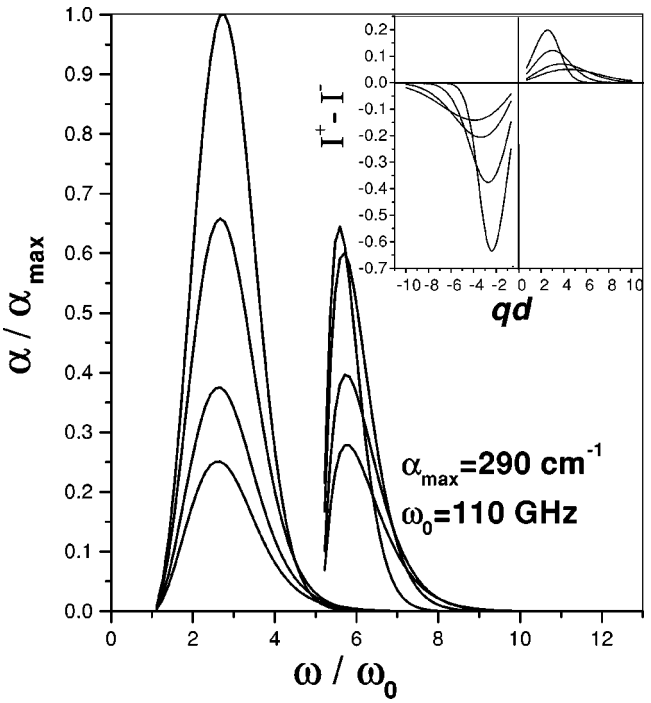

FIG. 5. The amplification coefficient versus frequency for the $Si/Si_{0.5}Ge_{0.5}/Si$ heterostructure. In the inset the population factor $\mathcal{I}^{(+)} - \mathcal{I}^{(-)}$ is presented as a function of qd. All curves calculated at $T = 50$, 100, 150, and 300 K. Amplitudes of all shown dependences decrease with increasing of temperature.

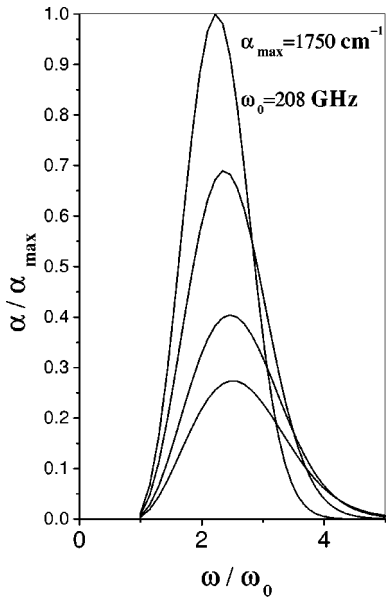

FIG. 6. The amplification coefficient versus frequency for the Si/Ge/Si heterostructure at $T=50$, 100, 150, and 300 K.

the second SSV phonon branch explains the smaller magnitude of α for this branch. For the first SSV branch, the maximum amplification is achieved for low temperatures: $\alpha_{max}(4\ \mathrm{K})=770\ \mathrm{cm}^{-1}$ and $\alpha_{max}(50\ \mathrm{K})=290\ \mathrm{cm}^{-1}$ at $\omega=300$ GHz. As temperature increases above 50 K, the amplification coefficient decreases, but at $T=300$ K it is still high: $\alpha_{max}(300\ \mathrm{K})\approx 80\ \mathrm{cm}^{-1}$. For the second SSV phonon branch, the maximum amplification occurs at $\omega\approx 650$ GHz. In the temperature range from 50 to 100 K, the maximum amplification coefficient is almost constant ($\approx 190\ \mathrm{cm}^{-1}$) and decreases for $T>100$ K. At room temperature, the values of α for both amplification bands are almost equal.

To demonstrate that even larger amplification effects can be achieved, we also calculated $\alpha(\omega)$ for another *p*-doped SiGe heterostructure: a 50-Å Ge QW embedded between Si layers.[22] The results are presented in Fig. 6 for different temperatures. The parameters of both materials and the carrier concentration were selected as described above. The frequency is measured in units of $\omega_0=208$ GHz. One can see that the amplification is larger than in the previous case, particularly, $\alpha_{max}(50\ \mathrm{K})=1750\ \mathrm{cm}^{-1}$ at $\omega=460$ GHz. The larger values of α are due to both the thinner QW layer and the larger acoustical mismatch (better phonon confinement).

V. DISCUSSION AND CONCLUSION

In low-dimensional structures, where electrons (holes) are confined in a quantum well, or in a quantum wire, drifting electrons generate both bulklike and confined acoustic phonons. Both types of phonons contribute, say, to the limitation of the carrier mobility and many other effects. The lack of the electron-phonon coupling strength for the bulklike phonons is compensated by their dominant density of states. For the amplification of a particular phonon mode, however, the coupling between this mode and the carriers is extremely important. Indeed, generally, the Čerenkov effect holds for all phonons, if the carrier drift velocity exceeds the phase velocity of these phonons. However, realization of a measurable phonon amplification is possible only for those phonons which are strongly coupled to the carriers. Low-dimensional carriers are coupled strongly only with the confined phonon modes.

Phonon confinement exists if velocities of the acoustic waves satisfy the inequality (1). Using the data on the elastic moduli and the material densities given in Refs. 21,23 and 24, it can be proved easily that most of the QW heterostructures made from III-V, II-VI, and IV-VI compounds, as well as SiGe materials, meet this condition and both carriers and phonons can be confined within the same QW layer.

In previous sections, we have developed a quantum approach to describe the confined phonon modes and the Čerenkov effect of the phonon generation. The drifting electrons have been described by the shifted Fermi distribution, which is proved to be valid for strong electron-electron scattering.[17,25] In this approach, three electron parameters—concentration, temperature, and drift velocity—must be specified to determine the Čerenkov effect. Then, we have demonstrated that acoustical phonons confined within a QW layer can be amplified and generated by the drift of the two-dimensional carriers in this layer.

The simple analytical model presented in Sec. III demonstrated the general properties of this effect. The effective electron-phonon coupling is strongly dependent on the phonon confinement and it increases significantly in the high-frequency (high-wave vector) range. On the other hand, the electrons can interact with phonons of wave vectors having an upper limit of $2k_F$ (for degenerated carriers), or of approximately $2\sqrt{2m^*k_BT}/\hbar$ (for nondegenerated carriers). These two factors result in the existence of a narrow amplification band with a sharp maximum of the amplification coefficient for each of the confined phonon branches interacting with the carriers. The simple model suggests a high value of the amplification coefficient (above $10^3\ \mathrm{cm}^{-1}$) in the sub-THz frequency range.

Using the general equations of Sec. II, we have performed the calculations of the confined modes and the amplification effect for strained SiGe QW heterostructures. Contemporary SiGe technology is developed well enough to fabricate different high-quality pseudomorphic SiGe heterostructures; see, for example, Ref. 26. For the symmetric heterostructures sketched in Fig. 1 we have found that only symmetric shear vertical modes interact with the carriers. The SiGe heterostructures are characterized by the acoustic velocities satisfying the inequality (2). For such a case, all SSV phonon branches are *excited* and have the previously discussed onsets in frequencies (and wave vectors). We have considered the amplification effect due to the drift of the heavy holes confined in the SiGe layer. We showed that the amplification bands for the confined phonons in these structures are even more narrow than that appearing in the simple model. For the hole drift velocity, we suppose $V_{dr}=2.5\ V_{TA}=8.5\times 10^5$ cm/sec. In the case of the 100-Å $Si/Si_{0.5}Ge_{0.5}/Si$ QW heterostructure with a hole concentration of $10^{12}\ \mathrm{cm}^{-1}$, we found that two phonon branches can be amplified, as demonstrated in Fig. 5. For the 50-Å Si/Ge/Si QW structure, we found one phonon branch which can be amplified by the drift of the carriers. The frequencies of amplified phonons

are in the sub-THz range and the amplification coefficient is of the order of hundreds to thousands of cm^{-1}.

We suggest the use of modulation-doped SiGe structures with a high hole mobility. In this case, the necessary values of the drift velocities (above 5×10^5 cm/sec) can be achieved in modest electric fields. Our calculations for different electron temperature have shown that though the amplification effect decreases at high temperatures, the amplification coefficient remains high enough at temperatures of about 300 K. Our estimates have shown that at higher temperatures, amplification of the higher phonon branches becomes dominant. Moreover, due to dependence of the effect on the population factor, the amplification associated with these branches can even increase with increasing of temperature.

In any structure, besides the amplification caused by the carriers, there always exist phonon losses due to scattering by imperfections. There are also unavoidable phonon losses due to the effects of anharmonicity and scattering on isotopes. The latter losses were estimated in Refs. 27 and 28. According to the data of these papers, in the sub-THz range the phonon losses due to the anharmonicity and scattering by isotopes are well below the calculated amplification coefficients of the present work. Thus, at least in perfect structures, the amplification of the confined modes exceeds their losses considerably.

The Čerenkov effect studied in this paper can be used for both the amplification of a given high-frequency acoustic signal and the generation of a high-frequency phonon flux. We suggest that in modulation-doped high-mobility heterostructures a large amplification effect can be achieved in modest electric fields. The simplest device for phonon generation is a single passage device. The condition of phonon generation in such a device,

$$\alpha L_x \gg 1, \tag{41}$$

can be realized for reasonable extensions of the structure L_x, since the predicted values of α are large. In the framework of the linear analysis developed above the distribution of the phonon flux intensity can be found to be proportional to $\exp[\alpha(\omega)L]$. Under condition (41) the latter means that the device generates a flux of phonons propagating along the applied field with a very narrow frequency distribution around the maximum of $\alpha(\omega)$, i.e., a flux of almost coherent phonons. It is important that the generated short-wavelength phonon beam has to be highly collimated. Indeed, for the example of the Si/SiGe/Si structure, at the maximum of amplification the generated phonon flux is confined to a spatial region of thickness of about 200 Å (the phonon wavelength is 160 Å).

In conclusion, we have found that the drift of two-dimensional electrons in the QW's lead to the instability of phonon subsystem: the phonon modes confined within the QW layer and propagating along the electron flux are amplified. The amplification coefficient for each of these modes has a sharp maximum in the sub-THz frequency range. The maximum values of the amplification coefficient are of the order of 100 to 10^3 cm^{-1}.

The Čerenkov effect studied here comprises such phenomena as strong electron-confined phonon coupling, high electron densities, and high electron mobilities in QW structures, and can be used for both the amplification of a given high-frequency acoustic signal and the generation of a high-frequency phonon flux. As a result of the phonon confinement effect it is predicted that the a high-collimated phonon beam can be generated. Thus, a simple electrical method for generation of high-frequency coherent phonons can be developed on the basis of the Čerenkov effect.

ACKNOWLEDGMENTS

This work was supported by the grant of Ukrainian State Foundation for Fundamental Researches and the US Army Research Office.

APPENDIX

To account for the electron screening effect on the electron-phonon interaction, one can use the fact that electron motion is much faster than that of the lattice. In quantitative terms, this results in the following condition: $V_{el} \gg V_{LM}, V_{TM}$, where V_{el} is the average electron velocity. This inequality always holds for semiconductors. Thus, electrons adiabatically follow acoustic phonons and the screening can be estimated in the static approximation. The electron-phonon interaction energy H_{int} induces an electron redistribution and an electrostatic potential $\phi^{(ind)}$, so that the total perturbation energy is

$$H_{int}^{(scr)} = H_{int} - e\phi^{(ind)}. \tag{A1}$$

To calculate $\phi^{(ind)}$ we find the perturbed electron wave function

$$\tilde{\Psi}_{1,\vec{k}} = \frac{1}{\sqrt{L_x L_y}}\chi_1(z)e^{i\vec{k}\cdot\vec{r}} + \frac{1}{\sqrt{L_x L_y}}\chi_1(z)\sum_{\vec{k}'}\frac{H_{int,11}^{(scr)}(\vec{k}-\vec{k}')}{E(\vec{k})-E(\vec{k}')}e^{i\vec{k}'\cdot\vec{r}}, \tag{A2}$$

where

$$H_{int,11}^{(scr)}(\vec{k}-\vec{k}') \equiv \frac{1}{L_x L_y}\int dz \int dx dy \chi_1^2(z) H_{int}^{(scr)}(\vec{r},z)e^{i\vec{k}\cdot\vec{r}}$$

and the one-subband approximation is assumed. The induced changes in the charge density are

$$\rho^{(ind)}(\vec{r},z) = -2e\sum_{\vec{k}}\left\{\left|\tilde{\Psi}_{1,\vec{k}}(\vec{r})\right|^2 - \frac{1}{L_x L_y}\chi_1^2(z)\right\}F(\vec{k}) = -e\chi_1^2(z)\sum_{\vec{q}} A_{11,q} H_{int,11}^{(scr)}(q)e^{i\vec{q}\cdot\vec{r}}. \tag{A3}$$

The solution of Poisson's equation with this charge density is

$$\phi^{(ind)}(\vec{r},z)=\frac{1}{\kappa}\int dz\int d\vec{r}\frac{\rho^{(ind)}(\vec{r}',z')}{\sqrt{(\vec{r}-\vec{r}')^2+(z-z')^2}}. \tag{A4}$$

Using the two-dimensional Fourier transformation of the Coulomb interaction

$$\frac{1}{\sqrt{(\vec{r}-\vec{r}')^2+(z-z')^2}}=\frac{2\pi}{L_xL_y}\sum_{\vec{q}}\frac{1}{q}e^{i\vec{q}\cdot(\vec{r}-\vec{r}')}e^{-q|z-z'|},$$

we calculate straightforwardly

$$\phi^{(ind)}(\vec{q},z)=\frac{2\pi e}{\kappa}A_{11}(\vec{q})H^{(scr)}_{int,11}(\vec{q})\frac{1}{q}\int dz'\chi^2(z')e^{-q|z-z'|}.$$

According to Eq. (8), probabilities of transitions are determined by matrix elements calculated with wave functions $\chi_1(z)$. In particular, we find

$$-e\phi^{(ind)}_{11}(\vec{q})=\frac{2\pi e^2dA_{11}(q)\mathcal{B}(qd)/\kappa}{1+2\pi e^2dA_{11}(q)\mathcal{B}(qd)/\kappa}H^{(scr)}_{int,11}(q) \tag{A5}$$

with factors $A_{11}(q)$ and $\mathcal{B}(qd)$ given by Eqs. (12) and (13). Using these results and Eq. (A1) we can easily calculate $H^{(scr)}_{int,11}(q)$ and prove the substitution represented by Eq. (10).

For a QW with infinite barriers, the factor $\mathcal{B}$ can be found explicitly:

$$\mathcal{B}(s)=\frac{1}{2}\frac{3s^5+5s^3\pi^2+2s\pi^4-\pi^4+e^{(-2s)}\pi^4}{s^3(s^2+\pi^2)^2}. \tag{A6}$$

One can see that the function $\mathcal{B}(s)\propto 1/s$ for $s\ll 1$, $\mathcal{B}(1)=0.69$ and $\mathcal{B}(s)\ll 1$ for $s>1$.

[1] W. A. Kutt, W. Albrecht, and H. Kurz, IEEE J. Quantum Electron. **QE-28**, 2434 (1992).

[2] R. Merlin, Solid State Commun. **102**, 207 (1997).

[3] H. N. Lin, R. J. Stoner, and H. J. Maris, J. Nondestruct. Eval. **9**, 239 (1990).

[4] Y. Iwazaki, T. Mishina, Y. Masumoto, and M. Nakayama, in *Proceedings of the 23rd International Conference on the Physics of Semiconductors*, edited by M. Scheffler and R. Zimmerman (World Scientific, Singapore, 1996), p. 701.

[5] C. K. Sun, J. C. Liang, C. J. Stanton, A. Abare, L. Coldren, and S. P. DenBaars, Appl. Phys. Lett. **75**, 1249 (1999).

[6] X. Hu and F. Nori, Physica B **263-264**, 16 (1999).

[7] A direct experiment on stimulated emission of 50-GHz acoustic phonons under optically driven population inversion of impurity electron levels in ruby was recently reported in H. W. de Wijn, P. A. van Walree, and A. F. M. Arts, Physica B **263-264**, 30 (1999).

[8] J. Faist, F. Capasso, D. L. Silco, C. Sirtori, A. L. Hutchinson, and A. Y. Cho, Science **264**, 553 (1994).

[9] Stimulated generation of THz plasmons in the three-barrier structure was recently observed in P. Bakshi, K. Kempa, A. Scorupsky, C. G. Du, G. Feng, R. Zobl, G. Strasser, C. Rauch, Ch. Pacher, K. Unterrainer, and E. Gornik, Appl. Phys. Lett. **75**, 1685 (1999).

[10] B. A. Glavin, V. A. Kochelap, and T. L. Lynnyk, Appl. Phys. Lett. **74**, 3525 (1999).

[11] J. H. McFee, in *Physical Acoustic*, edited by W. P. Masson (Academic, New York, 1966), Vol. IV, p. 1.

[12] V. V. Mitin, V. A. Kochelap, and M. A. Stroscio, *Quantum Heterostructures* (Cambridge University Press, New York, 1999).

[13] L. Wendler and V. G. Grigoryan, Surf. Sci. **206**, 203 (1988).

[14] L. D. Landau and E. M. Lifschitz, *Theory of Elasticity* (Pergamon, Oxford, 1986).

[15] Our solutions $\vec{u}_{\nu q}$ are presented in complex form; while computing Eq. (6) one needs to use $\mathrm{Re}\,\vec{u}_{\nu q}$.

[16] G. Bastard, *Wave Mechanics Applied to Semiconductor Heterostructures* (Halsted, Cedex, France, 1988).

[17] D. K. Ferry, *Semiconductors* (Macmillan, New York, 1991).

[18] V. A. Kochelap and V. V. Mitin, Phys. Rev. B **55**, 10 707 (1997).

[19] Notice, while the displacement $\vec{u}$ and the interface force σ_{zi} are continuous at an interfaces the relative volume change $\mathrm{div}\,\vec{u}$, as well as the torsional component $\mathrm{rot}\,\vec{u}$, in general, are discontinued.

[20] F. I. Fedorov, *Theory of Elastic Waves in Crystals* (Plenum, New York, 1968).

[21] O. Madelung, *Semiconductors. Group IV and III-V Compounds* (Springer, Berlin, 1991).

[22] A stable pseudomorphic Si/Ge/Si heterostructure can be grown on a graded buffer SiGe layer, when Si and Ge layers are strained.

[23] S. Adachi, J. Appl. Phys. **58**, R1 (1985).

[24] O. Madelung, *Semiconductors. Other than Group IV and III-V Compounds* (Springer, Berlin, 1992).

[25] Direct Monte Carlo calculations for two-dimensional electrons show that shifted Fermi-Maxwellian distributions are good approximations for the distribution function. See, for example, W. Xu, F. M. Peeters, and J. T. Devreese, Phys. Rev. B **43**, 14 134 (1991); G. Paulavicius, V. V. Mitin, and N. A. Bannov, J. Appl. Phys. **82**, 5580 (1997).

[26] H. G. Grimmeiss and J. Olajos, Phys. Scr. **T69**, 52 (1997).

[27] S. Tamura, Phys. Rev. B **30**, 849 (1984).

[28] S. Tamura, Phys. Rev. B **31**, 2574 (1985).